Multilayer Structures in Lipid Monolayer Films Containing Surfactant Protein C: Effects of Cholesterol and POPE

Stefan Malcharek, Andreas Hinz, Lutz Hilterhaus, and Hans-Joachim Galla
Institut für Biochemie, Westfälische Wilhelms-Universität Münster, D-48149 Münster, Germany

ABSTRACT The influence of cholesterol and POPE on lung surfactant model systems consisting of DPPC/DPPG (80:20) and DPPC/DPPG/surfactant protein C (80:20:0.4) has been investigated. Cholesterol leads to a condensation of the monolayers, whereas the isotherms of model lung surfactant films containing POPE exhibit a slight expansion combined with an increased compressibility at medium surface pressure (10–30 mN/m). An increasing amount of liquid-expanded domains can be visualized by means of fluorescence light microscopy in lung surfactant monolayers after addition of either cholesterol or POPE. At surface pressures of 50 mN/m, protrusions are formed which differ in size and shape as a function of the content of cholesterol or POPE, but only if SP-C is present. Low amounts of cholesterol (10 mol %) lead to an increasing number of protrusions, which also grow in size. This is interpreted as a stabilizing effect of cholesterol on bilayers formed underneath the monolayer. Extreme amounts of cholesterol (30 mol %), however, cause an increased monolayer rigidity, thus preventing reversible multilayer formation. In contrast, POPE, as a nonbilayer lipid thought to stabilize the edges of protrusions, leads to more narrow protrusions. The lateral extension of the protrusions is thereby more influenced than their height.

INTRODUCTION

The prerequisite for functional lung breathing is a reduced surface tension inside the alveoli. A thin lung surfactant film, which in human covers nearly 100 m^2 in size, is responsible for a low surface tension at the air/water interface. Lung surfactant consists of ~90% (w/w) lipids, mainly phospholipids, and 10% proteins. Four specific surfactant proteins are known, two hydrophilic (SP-A and SP-D) and two hydrophobic ones (SP-B and SP-C). Surface active components of the LS are, however, mainly SP-B and SP-C. The importance of the hydrophobic protein fraction has been demonstrated by knockout mice. SP-B deficiency proved to be lethal for animals (Akinbi et al., 1997), whereas results from SP-C knockout animals show pulmonary disorder associated with emphysema, monocytic infiltration, and epithelial cell dysplasia (Glasser et al., 2003). Congenital alveolar proteinosis with a hereditary SP-B deficiency results in a lack of tubular myelin (Claypool, 1988) and an increased formation of SP-C precursors (Nogee et al., 1993; Vorbroker et al., 1995). Of the phospholipids within the LS, ~80% are phosphatidylcholines, and ~50% of them contain the saturated palmitoic acid chains (DPPC) (Kahn et al., 1995).

Pure DPPC films can reach a surface tension near 0 mN/m during compression, but film formation is limited by a very slow adsorption of lipids from the subphase to the air/water-interface during expansion (Poulain and Clements, 1995; Robertson and Halliday, 1998; Veldhuizen and Haagsman, 2000).

It is presumed that the surface film within the alveolus is enriched with DPPC by selective adsorption from the subphase and/or a ''squeeze out'' of non-DPPC phospholipids during the breathing cycle (Goerke and Clements, 1986; Keough, 1992; Pison et al., 1996). Probably the components of surfactant films must collapse collectively rather than being squeezed out individually (Schief et al., 2003).

Although the natural LS film consists of more than one monolayer (Schürch et al., 1995), it is not clear which components of this film are involved in multilayer formation and the sustainment of such a film in vitro.

A number of phospholipids are found in very low concentrations in native surfactants (Veldhuizen et al., 1998). These minor lipid components, like *lyso*-phosphatidylcholine, phosphatidylserine, phosphatidylethanolamine, or *lyso*-bisphosphatidic-acid, have characteristic asymmetric structures. Partially unsaturated POPE, however, is able to form bilayers above the collapse pressure (Saulnier et al., 1999) and enhances the lateral mobility in various phosphatidylcholine lipid bilayers (Ahn and Yun, 1999).

The inclusion of these minor lipid components into the investigations of surfactant properties may lead to a better understanding of the mechanism, by which this complex biological surface active material interacts at the air/water interface. An important question is what correlations exist

Submitted August 2, 2004, and accepted for publication January 3, 2005.

Address reprint requests to Hans-Joachim Galla, E-mail: gallah@uni-muenster.de.

Abbreviations used: POPE, 1-palmitoyl-2-oleoyl-*sn*-glycero-3-phosphatidylethanolamine; β-BODIPY-PC, 2-(4,4-difluoro-5-methyl-4-boro-3a,4a-diaza-s-indacene-3-dodecanoyl)-1-hexadecanoyl-*sn*-glycero-3-phosphatidylcholine; DPPC, 1,2-dipalmitoyl-*sn*-glycero-3-phosphatidylcholine; DPPG, 1,2-dipalmitoyl-*sn*-glycero-3-phosphatidylglycerol; DPPE, 1,2-dipalmitoyl-*sn*-glycero-phosphatidylethanolamine; POPC, 1-palmitoyl-2-oleoyl-*sn*-glycero-3-phosphatidylcholine; DOPE, 1,2-dioleoyl-*sn*-glycero-3-phosphatidylethanolamine; DLPC, 1,2-dilauroyl-*sn*-glycero-3-phosphatidylcholine; LS, lung surfactant; SP, surfactant protein; FLM, fluorescence light microscopy; LB, Langmuir-Blodgett; SFM, scanning force microscopy.

0006-3495/05/04/2638/12 $2.00

doi: 10.1529/biophysj.104.050823

between the properties of asymmetric phospholipids and the properties of a mixture of the LS containing these lipids. Therefore, we have chosen POPE in different concentrations (0, 1, 10, and 30 mol %) as an example of asymmetric phospholipids and investigated their influence of the surface behavior on the LS model system consisting DPPC/DPPG/SP-C (80:20:0.4).

In mammalian species, cholesterol appears to be the major neutral lipid component (80–90%). The extracellular surfactant contains 3–10% cholesterol with respect to the total phospholipid (Veldhuizen and Haagsman, 2000). Due to its molecular structure cholesterol contributes to different functions such as stabilizing and fluidizing lipid mono- and bilayers (Smaby et al., 1997; Vist and Davis, 1990). Cholesterol can enhance adsorption of vesicles that are primarily composed of DPPC, presumably by increasing the fluidity of the condensed monolayer, thus improving film respreading (Fleming and Keough, 1988; Notter et al., 1980). However, it should be noted that cholesterol limits the minimum surface tension of the surface film as a result of an inhibited ''squeeze out'' of the sterol from DPPC/cholesterol monolayers (Notter et al., 1980; Yu and Possmayer, 1996; Yu and Possmayer, 1998). In binary monolayers with phosphatidylcholine, cholesterol changes the viscosity of monolayers (Tanaka et al., 1999) and influences protein adsorption due to strong interactions between phosphatidylcholine headgroups (Kim et al., 2001). The evolutionary analysis of surfactant composition revealed that fish lungs have ~3-fold greater amounts of cholesterol relative to phospholipids than other vertebrate groups (Daniels and Orgeig, 2003). In addition to the large evolutionary changes of the surfactant, temperature is also an acute controller of the lipid composition. Temperature-associated changes of cholesterol concentration in surfactant have previously been demonstrated in the Central Australian lizard, *Ctenophorus muchalis* (Daniels et al., 1990). It appears that at low body temperature the lungs of these animals increase the level of cholesterol in their surfactant to maintain the fluidity.

Previous studies have shown that SP-B and SP-C are involved in the formation of surface-associated reservoirs of lipid/protein multilayers (Krol et al., 2000; von Nahmen et al., 1997; Burns, 2003). Wilhelmy film balance, FLM, and SFM studies lead to a possible scenario of influences of SP-B and SP-C on the morphology of phospholipid monolayers: SP-B-containing films form disc-like protrusions with a thickness of one bilayer, whereas SP-C tends to form extended plateaus consisting of stacked bilayers. These stacked bilayers, which are found in the plateau region of the isotherms, are composed of phospholipids and SP-C (Bourdos et al., 2000), and show a layer thickness of 5.5–6.5 nm (Amrein et al., 1997; Galla et al., 1998; Krol et al., 2000; von Nahmen et al., 1997).

In this work, we focus on the influence of the components cholesterol and POPE on the morphology of mixed monolayers at different surface pressures in comparison to the LS model system. Upon compression cholesterol- and POPE-containing monolayers provide a range of structural changes that are visualized by means of SFM.

MATERIALS AND METHODS

Materials

SP-C was isolated from porcine lungs by the method described by Haagsman et al., 1987. DPPC, DPPG, and POPE were purchased from Avanti Polar Lipids (Alabaster, AL). BODIPY-PC was obtained from Molecular Probes (Eugene, OR) and cholesterol (>99% purity) from Sigma Aldrich Chemie (Steinheim, Germany). All lipids were used without further purification. Solvents were purchased from Merck (Darmstadt, Germany) and were of high-performance liquid chromatography grade.

Film balance measurements

Measurements were performed on a Wilhelmy film balance (built by Riegler and Kirstein, Mainz, Germany) with an operational area of 144 cm^2 on pure water (MilliQ quality, Milli-Q_{185}Plus; Millipore, Eschborn, Germany). All measurement were performed at a temperature of 20°C. Monolayers composed of DPPC/DPPG in a molar ratio of 4:1 were supplemented with 0.4 mol % SP-C as denoted. Different amounts of cholesterol or POPE were added as indicated. The lipid/protein mixtures were spread from a chloroform/methanol solution (1:1) onto the aqueous subphase. After an equilibrium time of 10 min, the monolayers were compressed at a rate of 5.81 cm^2/min.

Fluorescence light microscopy

Domain structures of lipid mixtures were visualized by means of a fluorescence light microscope (Olympus BX-FLA light microscope, equipped with an *xy*-stage; Olympus, Hamburg, Germany). All lipid and lipid/protein compositions were doped with 0.4 mol % BODIPY-PC.

Langmuir-Blodgett transfer

LB films were prepared by spreading a lipid/protein mixture dissolved in chloroform/methanol (1:1) onto a pure water subphase of a Wilhelmy film balance with an operational area of 39 cm^2. Before spreading, a mica sheet (Electron Microscopy Science, Munich, Germany) was dipped into the subphase. After an equilibration period of 10 min, the film was compressed with a velocity of 1.79 cm^2/min until the plateau region of the isotherms was reached (nearly 50 mN/m) and transferred onto the mica sheet (0.64 mm/min) under constant surface pressure. This was guaranteed by regulating the speed of the barrier manually. By using FLM, time-of-flight secondary ion mass spectrometry,, and Brewster angle microscopy it was shown that structures transferred from the air-water interface onto solid substrates are essentially identical (Galla et al., 1998; Lee et al., 1998; Leufgen et al., 1996).

Scanning force microscopy

Surface images of the LB films were obtained at ambient conditions using a Nanoscope IIIa Dimension 3000 microscope from Digital Instruments (Santa Barbara, CA) operating in tapping mode. Silicon tips (BS-Tap 300, Nanoscience Instruments, Phoenix, AZ) with a resonance frequency of 250–300 kHz were used.

Statistical analysis

FLM images were converted to 256 × 255 pixels and a resolution of 254 × 254 DPI, and decreased to a color depth of 8 BPP. Care was taken to keep a constant gain during the experiments. Owing to the inhomogeneous illumination of the monolayer by the light source, the intensities of the pixels

$I_{xy,raw}$ of the images were corrected. This was done by fitting a paraboloid to the image data and subtracting the paraboloid from the data. The corrected values of the intensities of the pixel I_{xy} at the locations (x, y) are given by

$$I_{xy} = I_{xy,raw} - M_x(x - x_0)^2 - M_y(y - y_0)^2, \quad (1)$$

where $I_{xy,raw}$ are the raw values, and M_x, M_y, x_0, and y_0 are fitted parameters characterizing the inhomogeneous illumination of the monolayer.

To calculate the areas A_d and A_b of the surface covered by the domains, the method described by von Nahmen and co-workers (1997) was used. The area of dark (d) and bright domains (b), and the mean fluorescence intensities $\overline{I_d}$ and $\overline{I_b}$ obtained from histograms of the fluorescence intensities were analyzed from digital images. The histograms could be fitted in most cases by a sum of two Gaussian functions (see Fig. 5 *a*). Each of the Gaussian funtions represents the intensity distribution of the dark $N_d(I)$ or bright domain $N_b(I)$. The parameters A_d, A_b, $\overline{I_d}$, and $\overline{I_b}$ were calculated from the integral and the means of the Gaussian distributions.

$$\frac{N(I)}{N_t} = \frac{1 - A_b^*}{\sigma_d\sqrt{\pi}}\exp\left\{-\frac{(I - \overline{I_d})^2}{\sigma_d^2}\right\} + \frac{A_b^*}{\sigma_b\sqrt{\pi}}\exp\left\{-\frac{(I - \overline{I_b})^2}{\sigma_b^2}\right\}. \quad (2)$$

$N(I)$ is the number of pixels with the intensity I, N_t the total number of pixels, $A_d^* = A_d/(A_d + A_b)$ and $A_b^* = A_b/(A_d + A_b)$ are the relative areas ($0 < A^* < 1$) of the dark and bright domains, and $\overline{I_d}$ and $\overline{I_b}$ are the corresponding mean intensities. The parameters σ_d and σ_b represent the width of the distributions.

SFM images were also converted to 256 × 255 pixels with a resolution of 254 × 254 DPI and decreased to a color depth of 8 BPP. Additionally, the SFM images were converted to a gray scale. To determine the parameters A_d^*, A_b^*, $\overline{I_d}$, and $\overline{I_b}$, which describe in the SFM images, the dark (d) area of the monolayer, the bright (b) area of the protrusions, and the mean height intensity of the protrusions ($\overline{I_b}$) and the monolayer $\overline{I_d}$, the histograms were analyzed as follows: up to a certain intensity I_{limit} the histograms were fitted by one Gaussian function yielding the parameters $\overline{I_d}$ and A_d^* (and $A_b^* = 1 - A_d^*$). The Gaussian function was then subtracted from the histogram, resulting in the intensity distribution of the bright domain N_b. Without knowledge of the concrete distribution function, an evaluation of the parameter $\overline{I_b}$ is then possible according to

$$\overline{I_b} = \frac{\sum_{I > I_{limit}} N_b I}{\sum_{I > I_{limit}} N_b}, \quad (3)$$

with N_b representing the number of pixels of the bright domains with the height intensity I. The applicability of the procedure was checked by changing the value of limit in a narrow range. No significant changes in the desired parameters were obtained.

For calculation of protrusion sizes shown with SFM, all adjacent pixels with similar color were figured up, whereas differences in gray scale not larger than 50 were accounted. That way, domain sizes, which are composed of many shades of single colors, have been determined.

RESULTS

Influence of cholesterol on model surfactant systems

Cholesterol leads to a shift of model surfactant isotherms to lower molecular areas as a result of an incorporation of cholesterol between the alkyl chains of the phospholipids (Fig. 1). The transition of lipids from the liquid-expanded (l_e) to the liquid-condensed (l_c) phase appears at a surface pressure of ~5 mN/m. SP-C-containing surfactant systems have a second plateau at a surface pressure of ~50 mN/m (Fig. 1 *b*), which is attributed to the collapse surface pressure of SP-C-containing monolayers. In contrast to the SP-C-free monolayers, the plateau of the lipid phase transition vanishes by increasing the amount of cholesterol. The SP-C-induced plateau at 50 mN/m, however, remains unaffected by the addition of cholesterol. Due to the incorporation of cholesterol, the monolayer stiffens in a more condensed manner compared to the cholesterol-free system.

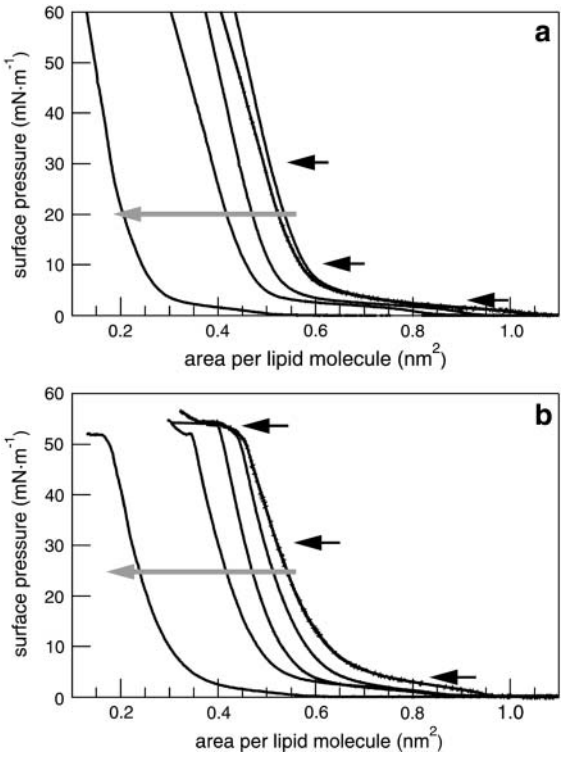

FIGURE 1 Compression isotherms of DPPC/DPPG (80:20) (*a*) and DPPC/DPPG/SP-C (80:20:0.4) (*b*) monolayers containing an increasing amount of cholesterol (*shaded arrow*). The concentrations of cholesterol are 0, 1, 5, 10, and 30 mol % of the total lipid amount. FLM images were taken at the surface pressures marked by black arrows.

In the fluorescence images of DPPC/DPPG (80:20) monolayers, dark kidney-shaped domains are visible, which form coherent l_c areas at high surface pressures (Fig. 2, *a*, *e*, and *i*). Addition of cholesterol leads to the formation of small circular structures and to a decrease of the total l_c area (Fig. 2, *b–d*) at low surface pressure. In the case of low concentrations of cholesterol (1% and 10%, Fig. 2, *f*, *g*, *j*, and *k*), fractal structures are observed during compression, whereas the number of circular domains remains unaffected in the case of high concentrations of cholesterol (30%) (Fig. 2, *h* and *l*). The l_c domains increase only in size but not in number. Cholesterol, which is known to disturb preferentially the tightly packed domains at high surface pressure, obviously causes an increase of the solubility of the fluorescence dye (Fig. 2, *i–l*).

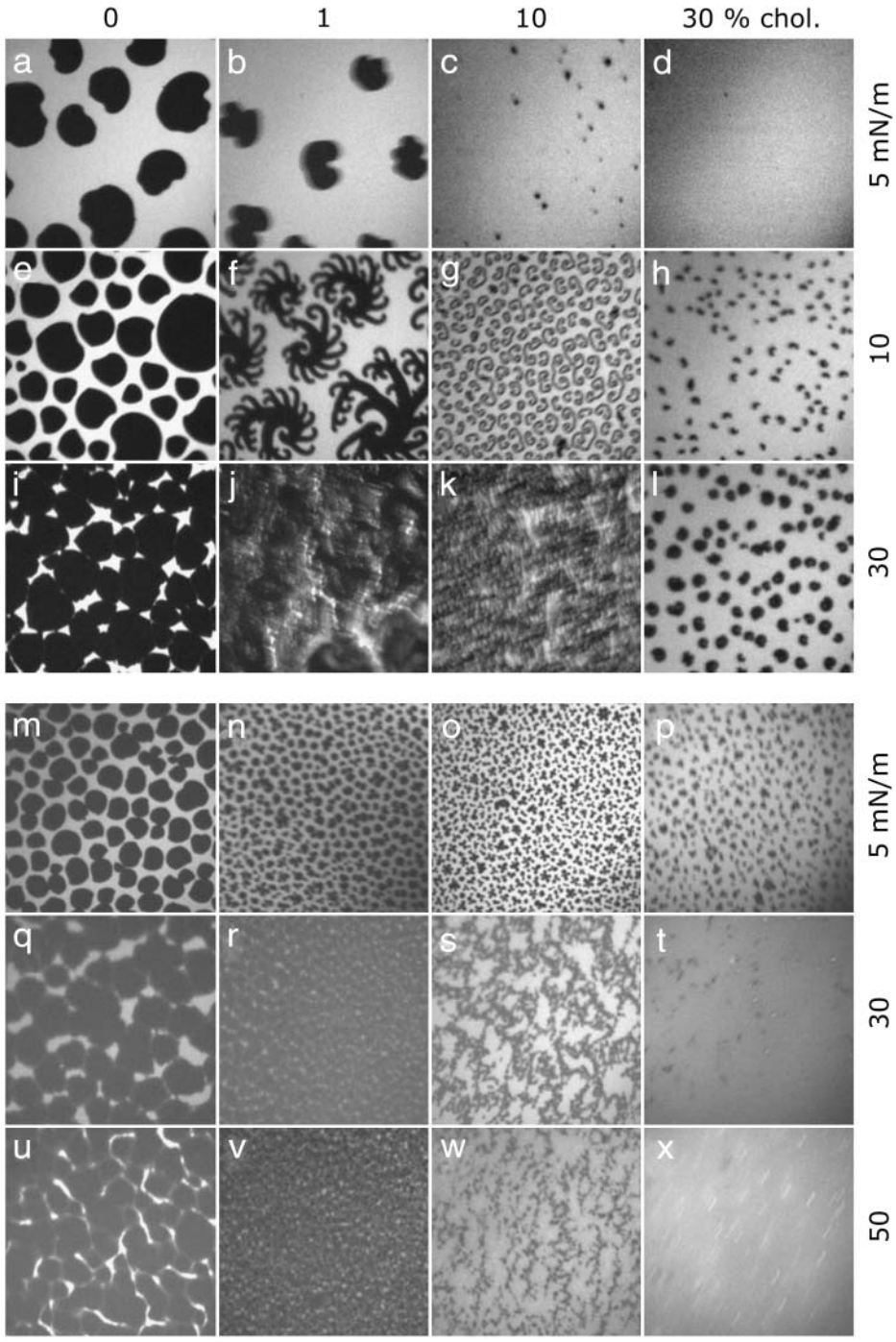

FIGURE 2 Fluorescence light microscopy images of DPPC/DPPG (80:20) (*a–i*) and of DPPC/DPPG/SP-C (80:20:0.4) (*m–x*) monolayers containing different amounts of cholesterol. Images were taken at surface pressures marked in Fig. 1. The concentrations of cholesterol are: 0 mol % (*first row*), 1 mol % (*second row*), 10 mol % (*third row*), and 30 mol % (*fourth row*). The image size is 130 × 130 μm^2.

FLM images of the model system DPPC/DPPG/SP-C (80:20:0.4) are similar to the protein-free system but exhibit some differences. Circular domains cover nearly the complete surface of all monolayers. At 5 mN/m and with increasing amounts of cholesterol the total area of the l_c phase decreases with respect to the l_e phase (Fig. 2, *m–p*). At higher surface pressures (30 and 50 mN/m) the l_e phase vanishes and the monolayers with lesser amounts of cholesterol are nearly in the condensed phase (Fig. 2, *q*, *r*, *u*, and *v*). A molar ratio of 10% cholesterol causes the formation of small circular domains that aggregate with long-range order (Fig. 2, *s* and *w*). At the highest content of cholesterol (30 mol %), the perturbation of the close-packed domains leads to an equal distribution of the fluorescence intensity that appears as a homogeneous phase (Fig. 2, *t* and *x*).

Influence of POPE on model surfactant systems

The isotherms of DPPC/DPPG (80:20) and DPPC/DPPG/SP-C (80:20:0.4) show an increasing compressibility during

compression between 10 and 20 mN/m at a constant area with increasing amounts of POPE (Fig. 3 *a*). The lipid phase transition from the l_e to the l_c phase is observed as a plateau at ~5 mN/m, which diminishes with an increasing amount of POPE. SP-C leads to the formation of a second plateau at 50 mN/m (Fig. 3 *b*). Due to the fluidizing effect of the unsaturated alkyl chain of POPE the lipid phase transition broadens and finally vanishes; this process is accompanied by a higher monolayer compressibility between 10 and 30 mN/m.

Addition of POPE to model surfactant systems leads to a fluidization of the monolayers visible by a quantitative reduction of l_c domains (Fig. 4, *a–c*) and a decrease in their size. Correspondingly, the area occupied by the l_e phase increases, leading to a higher compressibility of the monolayers. During compression, l_c domains grow in size and are either of circular or kidney-like shape (Fig. 4, *d–i*). At high surface pressures and at a low concentration of POPE (1 mol %), a network of l_c domains occurs, which is disrupted through further addition of POPE (Fig. 4, *g–i*). In general, the unsaturated alkyl chain of POPE promotes an incorporation of the fluorescence dye to give a bright domain surrounding single circular l_c domains.

SP-C leads to the formation of very small circular l_c domains, which partly aggregate (Fig. 4, *j–l*). At high surface pressures the contrast between dark l_c domains and bright l_e domains diminishes (Fig. 4, *m–r*). Nevertheless, a firm phase interface of the domains remains and l_c domains obviously consist of saturated lipids surrounded by POPE molecules. Accordingly, POPE molecules should stabilize the borders of l_c domains and the increasing l_e arrays are predominantly composed of POPE.

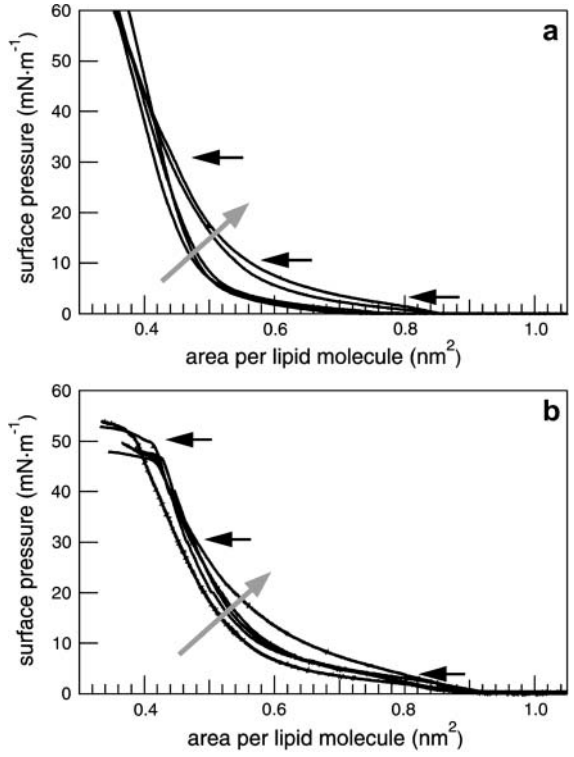

FIGURE 3 Compression isotherms of (*a*) DPPC/DPPG (80:20) and (*b*) DPPC/DPPG/SP-C (80:20:0.4) monolayers containing an increasing amount of POPE (*shaded arrow*). The concentrations of POPE are 0, 1, 5, 10, and 30 mol % of the total lipid amount. FLM images were taken at the surface pressures marked by black arrows.

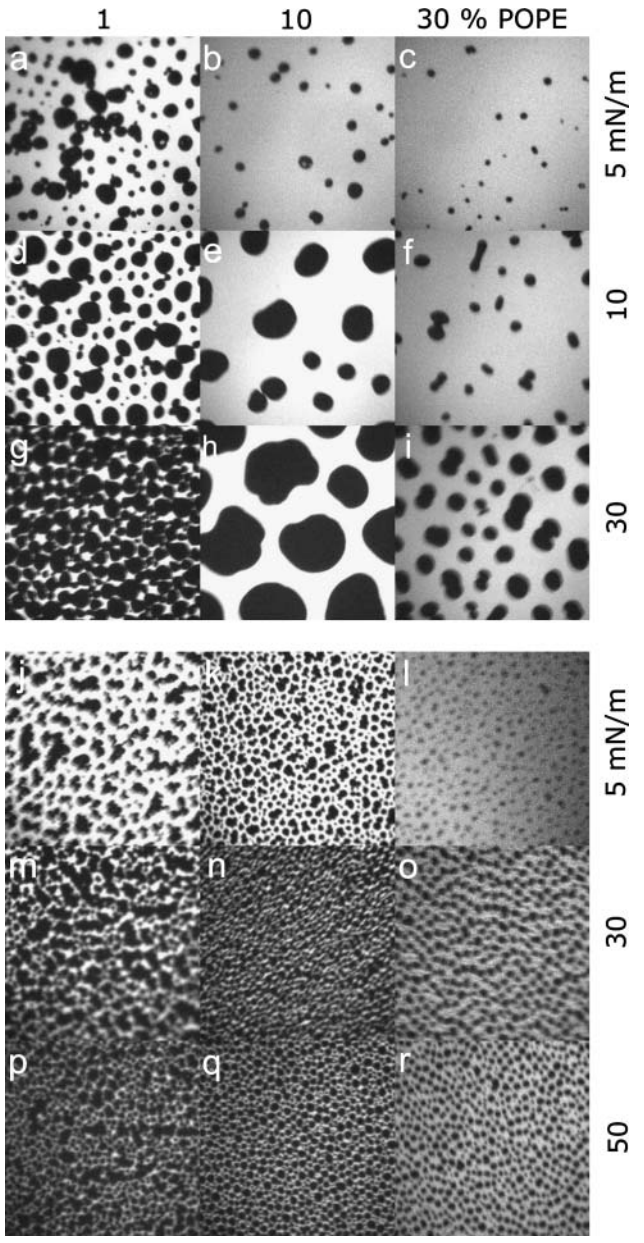

FIGURE 4 Fluorescence light microscopy images of DPPC/DPPG (80:20) (*a–i*) and of DPPC/DPPG/SP-C (80:20:0.4) (*m–x*) monolayers containing different amounts of POPE. Images were taken at surface pressures marked in Fig. 2. The concentrations of POPE are: 0 mol % (*first row*), 1 mol % (*second row*), 10 mol % (*third row*), and 30 mol % (*fourth row*). The image size is 130 × 130 μm^2.

Quantification of the influence of minor components on the phase behavior of model surfactant monolayers

The visual impression of FLM images was quantified by a statistical analysis. At a surface pressure of 5 mN/m the different surfactant model systems with various amounts of cholesterol or POPE were analyzed to quantitate the area occupied by the l_e and the l_c phases, respectively. Histograms of the FLM images indicate a normal distribution around a bright and a dark gray-scale value (Fig. 5 *a*). The solid lines represent the fitting of data as the sum of two Gaussian distributions (Eq. 2). The point of intersection of both normal distributions corresponds to the border between bright and dark phases, and the areas of the two phases were calculated by an integration of Gaussian distributions. Both minor components, cholesterol and POPE, lead to an increase of the ratio of bright and dark domains A_b^*/A_d^* (Fig. 5, *b* and *c*). The influence of cholesterol/POPE on the protein-free system DPPC/DPPG (80:20) is higher than the influence on DPPC/DPPG/SP-C (80:20:0.4). Cholesterol has a stronger influence on the protein-free surfactant system than POPE, but the addition of 0.4% SP-C leads to a drastic change. Addition of POPE to DPPC/DPPG/SP-C (80:20:0.4) monolayers amplifies the area of bright domains in comparison to cholesterol-containing membranes. Due to the unsaturated fatty acid, POPE is assumed to be responsible for the fluidization of the model lung surfactant monolayers, whereas cholesterol leads to the formation of a lower amount of l_c phase by an incorporation and disturbance of l_c phase.

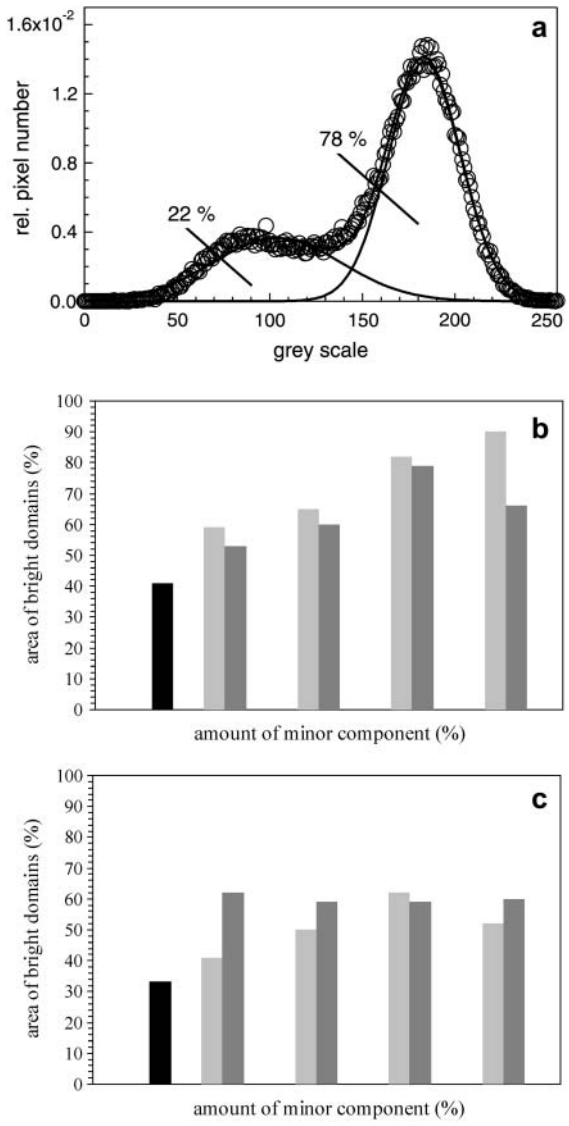

FIGURE 5 Statistical analysis of FLM images at a surface pressure of 5 mN/m. (*a*) The areas of bright and dark domains were calculated by fitting the data to the sum of two Gaussian distributions. The Gaussian curve with an area of 78% represents the l_e phase, whereas the other one marks the dark domains with a total area of 22%. (*b* and *c*) Histograms of fluorescence light intensity of (*b*) DPPC/DPPG (80:20) and (*c*) DPPC/DPPG/SP-C (80:20:0.4) monolayers with various amounts of cholesterol/POPE. Model surfactant system in black, cholesterol-doped in light shaded, and POPE-doped in dark shaded.

Topographical and height analysis

To consider the proposed three-dimensional model of the lung surfactant, the lipid/protein mixtures were transferred at a surface pressure of 47 mN/m by using a LB transfer to mica sheets and were examined by means of SFM (Galla et al., 1998). The model system DPPC/DPPG/SP-C (80:20:0.4) forms long filamentous protrusions (Fig. 6 *a*) in a long-range order (Fig. 7 *a*). A height analysis of these protrusions visualizes the formation of lipid bilayers up to a quadruple bilayer assuming a lipid bilayer thickness of ~6 nm (Table 1). SFM images of DPPC/DPPG/SP-C (80:20:0.4) with an additional amount of either 10% (Fig. 6 *b*) or 30% cholesterol (Fig. 6 *c*) reveal the formation of two types of distinct protrusions. With less amount of cholesterol numerous broad protrusions are formed, which supports the hypothesis that cholesterol stabilizes lipid double layers (Table 1). The protrusions exhibit one lipid bilayer. Partly, these protrusions consist of a protrusion of higher order leading to the formation of a second bilayer sitting on top of the first bilayer. With high amounts of cholesterol, most of the protrusions vanish; only isolated ones appear. These protrusions consist of a punctual structure with a maximum height of two bilayers. Furthermore, several protrusions appear, which are comparable with the structures existing at 10 mol %. In general, 30 mol % cholesterol inhibits multilayer formation. Therefore, the addition of cholesterol reduces the total number of stacks within the protrusions in comparison to the model system DPPC/DPPG/SP-C (80:20:0.4) (Table 1).

POPE induces the formation of small circular protrusions (Fig. 6 *d*) that decrease in size but increase in number upon further addition of POPE (Fig. 6 *e*, Table 1). The long-range order is characterized by long filaments that consist of many small protrusions interrupted by flat areas (Fig. 7 *c*). High amounts of POPE (30%) lead to the formation of separated

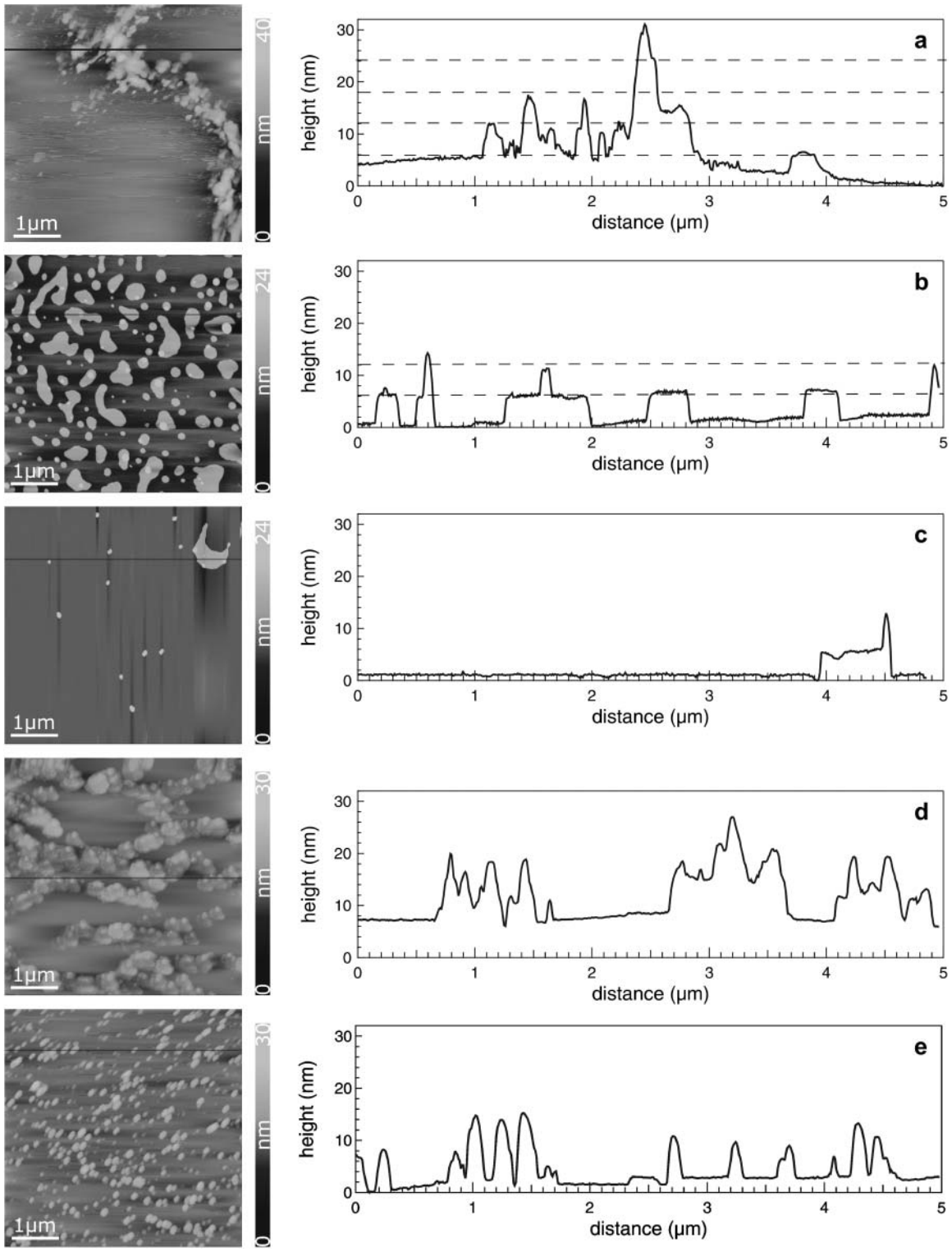

FIGURE 6 SFM images and height profiles of DPPC/DPPG/SP-C films containing different amounts of cholesterol/POPE. (*a*) 0 mol % of cholesterol/POPE, (*b*) 10 mol % of cholesterol, (*c*) 30 mol % of cholesterol, (*d*) 10 mol % of POPE, and (*e*) 30 mol % of POPE. The line scans exhibit the height profile. Protrusions are visualized as single steps of lipid bilayers. The image size is $5 \times 5\ \mu m^2$.

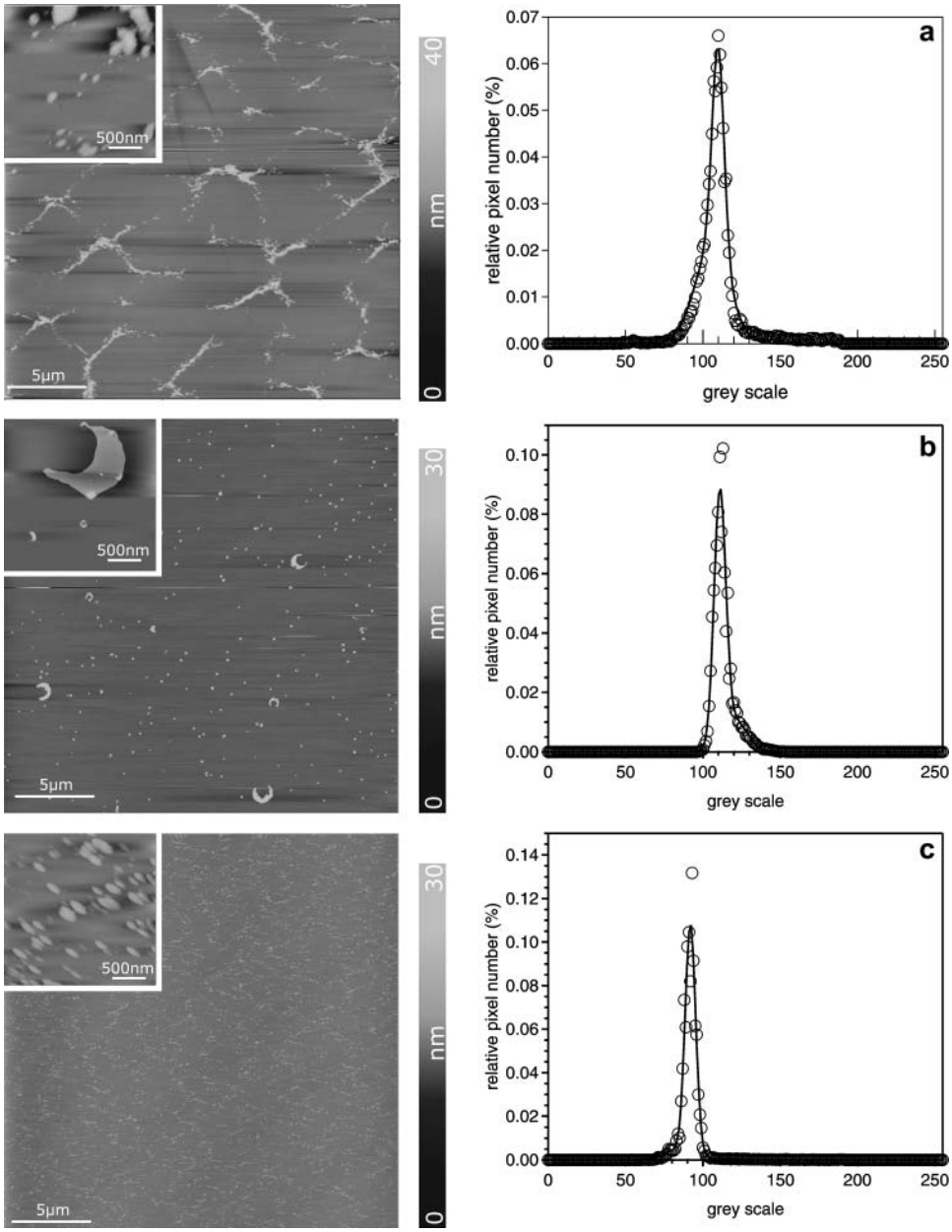

FIGURE 7 SFM images and histograms of the gray-scale analysis of model surfactant monolayers. (*a*) DPPC/DPPG/SP-C (80:20:0.4), (*b*) DPPC/DPPG/SP-C/ cholesterol (80:20:0.4:30), and (*c*) DPPC/DPPG/SP-C/POPE (80:20:0.4:30). The insets show magnifications of the protrusions with an image size of $2 \times 2\ \mu m^2$. The histogram analysis of the full-scale images represent fits to a Gaussian distribution. The image size is $25 \times 25\ \mu m^2$. Insets are $2 \times 2\ \mu m^2$.

protrusions, whereas their total area remains constant (Table 1). We conclude that this effect corresponds to an increasing relative surface of the edge of protrusions, which shows the rim-stabilizing effect of the nonbilayer lipid POPE.

DISCUSSION

This study focuses on the influence of cholesterol and POPE on a pure lipid, DPPC/DPPG (80:20), and on a lung surfactant model system, DPPC/DPPG/SP-C (80:20:0.4). The investigation contributes to a further understanding of the function of these so-called minor components in the alveolus during the breathing cycle.

Bilayer stabilizing effect of cholesterol

Film balance experiments indicate that cholesterol is incorporated between the alkyl chains of phospholipids, resulting in less required space compared to the expected space of alkyl chains as a sum of the pure components. This has also been reported by Kim et al. (2001) for cholesterol-doped DPPC and DPPG monolayers. The hydroxylic group of cholesterol interacts with the headgroups of DPPC and DPPG (Mozaffary, 1994), DLPC (Tanaka et al., 1999), and protein-containing monolayers such as DPPC/GM1 (Yuan and Johnston, 2000). The condensing effect of cholesterol leads to an ordered monolayer at concentrations >30 mol % cholesterol (Kim et al., 2001). Isotherms of mixed lipid/

TABLE 1 Topographical and height analysis of SFM images of surfactant model systems

Surfactant model system	Area of protusions (%)	Height steps of protrusions (nm)*
DPPC/DPPG/SP-C (80:20:0.4)	20	6 (1), 12 (2), 18 (3), 24 (4)
DPPC/DPPG/SP-C/cholesterol (80:20:0.4:10)	27	6 (1), 12 (2)
DPPC/DPPG/SP-C/cholesterol (80:20:0.4:30)	5	6 (1), 12 (2)
DPPC/DPPG/SP-C/POPE (80:20:0.4:10)	23	6 (1), 12 (2), 18 (3)
DPPC/DPPG/SP-C/POPE (80:20:0.4:30)	23	6 (1), 12 (2), 18 (3)

*Data in parentheses represent the number of bilayers.

cholesterol monolayers show a great analogy to those of pure cholesterol. At higher concentrations of cholesterol no uniform mixture is observed. An increase in rigidity resulting from the condensing effect of cholesterol was shown by plotting the area per molecule versus the cholesterol content at constant pressure (Tanaka et al., 1999). The observed values are below the calculated ones for an ideal mixture; thus, the density of mixed lipid/cholesterol monolayers is higher than the sum of the densities of the individual components.

Small amounts of surface active proteins should lead to only minimal changes (Yuan and Johnston, 2000). At low surface pressure the isotherms of DPPC/DPPG/SP-C (80:20:0.4) show a phase behavior similar to the pure lipid monolayer, exhibiting the shift to smaller molecular areas with rising concentration of cholesterol. At higher surface pressures, ~50 mN/m, SP-C leads to the reversible formation of a plateau (von Nahmen et al., 1997), which is not affected by cholesterol. At high concentrations of cholesterol, repeated compression and expansion cycles do not lead to a significant loss of material. By increasing the amount of cholesterol only the phase transition between l_e and l_c vanishes, indicating a disturbing effect of cholesterol within l_c domains due to its incorporation between the alkyl chains of the phospholipids. The orientation of these alkyl chains within different phases is hindered by cholesterol.

At low surface pressures, fluorescence images of DPPC/DPPG monolayers are characterized by kidney-shaped l_c domains within the l_e phase. Further compression leads to higher amounts of l_c domains and a decreased area of the l_e phase. Fluorescence images of DPPC/DPPG monolayers containing higher amounts of cholesterol exhibit a lower area of l_c phase, which was also reported by Worthman et al. (1997). A cholesterol-rich phase segregates ordered domains that exclude the fluorescence dye. At high surface pressures, the disaturated phospholipids form condensed domains that are depleted of the fluorescence dye. Cholesterol compensates this condensing effect of phospholipids under surface pressure, leading to a decreased area of l_c phase wherein the fluorescence dye is not soluble. Tanaka et al. (1999) made similar observations while investigating DLPC/cholesterol mixtures. Cholesterol induces a superstructure, preventing domain formation (Somerharju et al., 1985; Virtanen et al., 1995). This model is based on the assumption that each cholesterol molecule replaces a single acyl chain of phospholipids in their hexagonal lattice, and cholesterol perturbs this lattice due to its larger size. This perturbation is minimized by a maximal separation of cholesterol molecules, which can only be achieved by a hexagonal or centered rectangular superlattice of cholesterol molecules.

Fluorescence images of cholesterol-containing DPPC/DPPG/SP-C (80:20:0.4) monolayers reveal substantially smaller circular l_c domains compared to those of DPPC/DPPG (80:20). These domains form a nearly uniform l_c area in the plateau region, interrupted by small l_e arrays. These l_e arrays consist of less-ordered alkyl chains in which the fluorescence dye is incorporated (Lösche and Möhwald, 1984; Nag et al., 1990; Helm and Möhwald, 1988). Within these l_e arrays protrusions are present, and their formation is supported by SP-C (von Nahmen et al., 1997). SP-C reduces the size of individual l_c domains at a constant total area of l_c phase. This leads to an increase of the total length of the interface between the l_e and l_c phases. The protrusions consist of stacked bilayers, each with a thickness of 6 nm. They appear as single steps in the height profile of SFM images (Fig. 6). A long-range order of protrusions is characterized by long, bright arrays of protrusions with varying size and height enclosing flat and round structures. These round structures represent the l_c phase consisting primarily of condensed DPPC (Bourdos et al., 2000). In the presence of cholesterol, protrusions cover a larger area of the surface, indicating a positive effect of cholesterol on the formation of lipid bilayers. Incorporation of cholesterol leads to a minimization of the length of the phase interface between the l_e and l_c phases. This can be attributed to the line-active properties of cholesterol (Sparr et al., 1999).

Since SP-C is responsible for multilayer formation, and since the protrusions are uniformly distributed over the whole surface, we guess that the protein is also homogeneously distributed. For this reason the filamentous structures of the cholesterol-free model system disappear.

Taneva and Keough describe similar observations while investigating DPPC/SP-C/cholesterol mixtures. Cholesterol prevents SP-C from self-aggregating and leads to a better miscibility in the monolayer (Taneva and Keough, 1997). These homogeneously dispersed protrusions were also found by Diemel et al., who investigated DPPC/POPC/POPG/SP-C monolayers in the presence of up to 20 mol % cholesterol (Diemel et al., 2002). The authors suggest that a homogenous dispersion of surfactant lipids may facilitate lipid insertion into the monolayer. By increasing the amount of cholesterol up to 30 mol % the total number of protrusions decreases (Fig. 6 *c*). Separated very small multilayers appear; only a few large crescent-shaped bilayers are observed, which contain several multilayers (see Fig. 7 *b*, *inset*). Cholesterol seems to strengthen the interaction of SP-C with lipid and consequently

almost inhibits the squeeze-out from the monolayer (Taneva and Keough, 1997). Due to the tendency of cholesterol to maximize the distance between two molecules, a hexagonal symmetric cholesterol superlattice is formed (Virtanen et al., 1995), and the overall rigidity of the monolayer caused by cholesterol prevents the model surfactant films from forming multilayers. In cases where nearly every third molecule is cholesterol, the formation of micelle-like structures at the rim of the protrusions is considerably disturbed (Fig. 8). A medium amount of cholesterol (10%) has a bilayer-stabilizing effect that promotes protrusion formation, whereas a high amount of cholesterol (30%) inhibits multilayer formation by increasing the rigidity of the monolayer.

POPE promotes protrusion formation

POPE has a fluidizing effect on model surfactant monolayers, resulting in a higher lateral mobility (Ahn and Yun, 1999). Successive replacement of POPC by POPE leads to an increase of the lateral mobility within binary mixtures. Investigations of Saulnier et al. (1999) have shown that not only are the headgroups of lipids crucial for the fluidity of a monolayer, but also the character of the alkyl chains (Saulnier et al. 1999). The saturated palmitoyl chains of the DPPE lead to lesser fluidity than the unsaturated oleoyl chains of DOPE. A combination of unsaturated and saturated alkyl chains, present in POPE, leads to the highest fluidity. Binary mixtures of DPPE and DOPE lead to an increased fluidity comparable to that of POPE. These investigations are in excellent agreement with the results of our study of the model systems DPPC/DPPG/POPE (80:20:*x*) and DPPC/DPPG/SP-C/POPE (80:20:0.4:*x*) (*x* represents a concentration of the minor component of 1, 5, 10, or 30 mol %),, supporting the conclusion that POPE-containing monolayers are characterized by an increased compressibility and fluidity. These effects are observed as a decrease in number and a size reduction of l_c domains in FLM experiments. Due to its unsaturated fatty acid, POPE is not incorporated into the l_c domains; thus the lipid is enriched in the l_e phase. At lower concentrations, we propose an accumulation of POPE at the interface between l_e and l_c phases, whereas at high concentrations, l_e arrays preferentially consist of POPE. The unsaturated alkyl chain enables an incorporation of the fluorescence dye into POPE-rich phases and prevents a squeeze-out of the fluorescence dye at high surface pressures. Therefore, POPE leads to a higher amount of l_e phase.

In the presence of SP-C, POPE also has a fluidizing effect on the surfactant model system DPPC/DPPG/SP-C/POPE (80:20:0.4:*x*). SP-C induces the formation of protrusions and is itself responsible for a higher fluidity of the monolayer (Amrein et al., 1997). These multilayers are composed of folded lipid bilayers and protein molecules, enabling the retention of the fluorescence dye (von Nahmen et al., 1997). The filamentous structure of the model system DPPC/DPPG/SP-C (80:20:0.4) is identical to the POPE-containing systems, but with higher amounts of POPE the protrusions get smaller and the multilayer formation becomes rare. The number of protrusions increases, however, whereas the area covered by protrusions remains constant. We propose that POPE stabilizes the rim of protrusions due to its overall conical shape. In contrast, DPPC and DPPG are of cylindrical shape and therefore not able to stabilize the

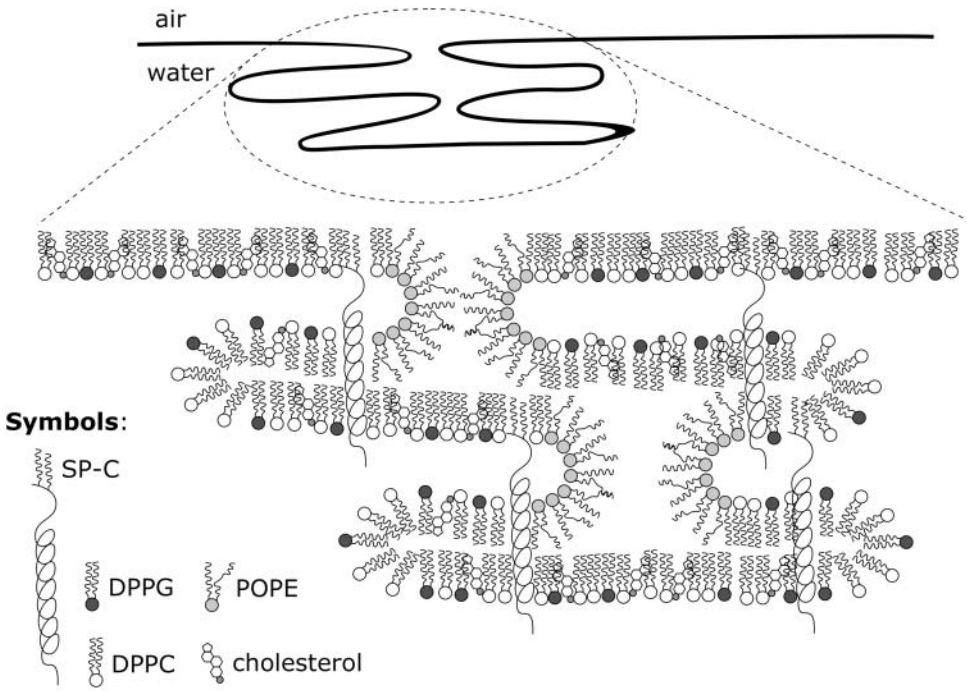

FIGURE 8 Proposed model of cholesterol/POPE interactions with the model surfactant system DPPC/DPPG/SP-C (80:20:0.4). POPE is enriched in the rims of the protrusions, whereas cholesterol stabilizes the bilayers.

rims of the protrusions. POPE seems to disperse large l_c into small l_c domains embedded in the fluid l_e phase.

The influence of POPE on the shape of protrusions is more pronounced than on their height (Fig. 6 *e*). In general, this influence on protrusion formation is attributed to two different effects. The lateral distribution within surfactant monolayers is changed in the way that the average size of SP-C-rich domains decreases with incorporated POPE. Due to its chemical, and thus topological, structure (conical shape), POPE stabilizes the interface between the l_e and l_c phases. This leads to an increase of the ratio of circumference to area. This effect is independent of the surface pressure. At high surface pressures POPE stabilizes the rims of protrusions, promoting a three-dimensional orientation of micelle-like structures (Fig. 8). Upon decreasing the molecular area, protrusions are formed underneath the monolayers (Plasencia et al., 2004), in which, probably, the hydrophilic headgroups of the first double layer face the hydrophilic headgroups of the next. The α-helix domain of SP-C should be incorporated in one bilayer (Pastrana et al., 1991; Vandenbussche et al., 1992), and the palmitoyl chains might stretch into the neighboring bilayer. In this picture, the fatty acids act as an anchor between adjacent bilayers, especially near the rims of the protrusions. In contrast, cholesterol stabilizes bilayers to give a flat surface. These findings suggest that the components cholesterol and POPE of the surfactant film influence the formation of the reversible multilayer structures and are relevant to stabilization of the lung during the breathing cycle.

This work was supported by the Deutsche Forschungsgesellschaft under grant Sonderforschungsbereich 424/B9.

REFERENCES

Ahn, T., and C. H. Yun. 1999. Phase properties of liquid-crystalline phosphatidylcholine/phosphatidylethanolamine bilayers revealed by fluorescent probes. *Arch. Biochem. Biophys.* 369:288–294.

Akinbi, H. T., J. S. Breslin, M. Ikegami, H. S. Iwamoto, J. C. Clark, J. A. Whitsett, A. H. Jobe, and T. E. Weaver. 1997. Rescue of SP-B knockout mice with a truncated SP-B proprotein. Function of the C-terminal propeptide. *J. Biol. Chem.* 272:9640–9647.

Amrein, M., A. von Nahmen, and M. Sieber. 1997. A scanning force- and fluorescence light microscopy study of the structure and function of a model pulmonary surfactant. *Eur. Biophys. J.* 26:349–357.

Bourdos, N., F. Kollmer, A. Benninghoven, M. Ross, M. Sieber, and H. J. Galla. 2000. Analysis of lung surfactant model systems with time-of-flight secondary ion mass spectrometry (TOF-SIMS). *Biophys. J.* 79: 357–369.

Burns, A. R. 2003. Domain structure in model membrane bilayers investigated by simultaneous atomic force microscopy and fluorescence imaging. *Langmuir.* 19:8358–8363.

Claypool, W. D. 1988. Pulmonary alveolar proteinosis. *In* Pulmonary Diseases and Disorders. A. P. Fishman, editor. McGraw-Hill, New York. 893–900.

Daniels, B. D., and S. Orgeig. 2003. Pulmonary surfactant: the key to the evolution of air breathing. *News Physiol. Sci.* 18:151–157.

Daniels, C. B., H. A. Barr, J. H. T. Power, and T. E. Nicholas. 1990. Body temperature alters the lipid composition of pulmonary surfactant in the lizard *Ctenophorus nuchalis*. *Exp. Lung Res.* 16:435–449.

Diemel, R. V., M. M. Snel, L. M. Van Golde, G. Putz, H. P. Haagsman, and J. J. Batenburg. 2002. Effects of cholesterol on surface activity and surface topography of spread surfactant films. *Biochemistry.* 41:15007–15016.

Fleming, B. D., and K. M. Keough. 1988. Surface respreading after collapse of monolayers containing major lipids of pulmonary surfactant. *Chem. Phys. Lipids.* 49:81–86.

Galla, H.-J., N. Bourdos, A. von Nahmen, M. Amrein, and M. Sieber. 1998. The role of pulmonary surfactant protein C during the breathing cycle. *Thin Solid Films.* 327–329:632–635.

Glasser, S. W., E. A. Detmer, M. Ikegami, C. L. Na, M. T. Stahlman, and J. A. Whitsett. 2003. Pneumonitis and emphysema in sp-C gene targeted mice. *J. Biol. Chem.* 278:14291–14298.

Goerke, J., and J. A. Clements. 1986. Alveolar surface tension and lung surfactant. *In* Handbook of Physiology. Section 3, The Respiratory System. Vol. 3, Mechanics of Breathing. A. P. Fishman, section editor. Peter T. Macklem and Jere Mead, volume editors. American Physiological Society, Bethesda, MD. 247–261.

Haagsman, H. P., S. Hawgood, T. Sargeant, D. Buckley, R. T. White, K. Drickamer, and B. J. Benson. 1987. The major lung surfactant protein, SP 28–36, is a calcium-dependent, carbohydrate-binding protein. *J. Biol. Chem.* 262:13877–13880.

Helm, C. A., and H. Möhwald. 1988. Equilibrium and nonequilibrium features determining superlattices in phospholipid monolayers. *J. Phys. Chem.* 92:1262–1266.

Kahn, M. C., G. J. Anderson, W. R. Anyan, and S. B. Hall. 1995. Phosphatidylcholine molecular species of calf lung surfactant. *Am. J. Physiol.* 269:567–573.

Keough, K. M. W. 1992. Physical chemistry of pulmonary surfactant in the terminal air space. *In* Pulmonary Surfactant: From Molecular Biology to Clinical Practise. B. Robertson, L. M. G. Van Golde, and J. J. Batenburg, editors. Elsevier, Amsterdam. 109–164.

Kim, K., C. Kim, and Y. Byun. 2001. Preparation of dipalmitoylphosphatidylcholine/cholesterol Langmuir-Blodgett monolayer that suppresses protein adsorption. *Langmuir.* 17:5066–5070.

Krol, S., M. Ross, M. Sieber, S. Kunneke, H. J. Galla, and A. Janshoff. 2000. Formation of three-dimensional protein-lipid aggregates in monolayer films induced by surfactant protein B. *Biophys. J.* 79:904–918.

Lee, K. Y. C., M. M. Lipp, J. A. Zasadzinski, and A. J. Waring. 1998. Direct observation of phase and morphology changes induced by lung surfactant protein SP-B in lipid monolayers via fluorescence, polarized fluorescence, Brewster angle and atomic force microscopies. *SPIE.* 3273:115–133.

Leufgen, K. M., H. Rulle, A. Benninghoven, M. Sieber, and H.-J. Galla. 1996. Imaging time-of-flight secondary ion mass spectrometry allows visualization and analysis of coexisting phases in Langmuir-Blodgett films. *Langmuir.* 12:1708–1711.

Lösche, H., and H. Möhwald. 1984. Fluorescence microscopy on monomolecular films at an air/water interface. *Colloids and Surfaces.* 10:217–240.

Mozaffary, H. 1994. Cholesterol-phospholipid interaction: a monolayer study. *Thin Solid Films.* 244:874–877.

Nag, K., C. Boland, N. H. Rich, and K. M. W. Keough. 1990. Design and construction of an epifluorescence microscopic surface balance for the study of lipid monolayer phase transitions. *Review of Scientific Instruments.* 61:3425–3430.

Nogee, L. M., D. E. DeMello, L. P. Dehner, and H. R. Colten. 1993. Deficiency of pulmonary surfactant protein B in congenital alveolar proteinosis. *N. Engl. J. Med.* 328:406–410.

Notter, R. H., S. A. Tabak, and R. D. Mavis. 1980. Surface properties of binary mixtures of some pulmonary surfactant components. *J. Lipid Res.* 21:10–22.

Pastrana, B., A. J. Mautone, and R. Mendelsohn. 1991. Fourier transform infrared studies of secondary structure and orientation of pulmonary surfactant SP-C and its effect on the dynamic surface properties of phospholipids. *Biochemistry.* 30:10058–10064.

Pison, U., R. Herold, and S. Schürch. 1996. The pulmonary surfactant system: biological function, components, physicochemical properties and alteration during lung diseases. *Colloids Surf. A.* 114:165–184.

Plasencia, I., L. Rivas, K. M. Keough, D. Marsh, and J. Perez-Gil. 2004. The N-terminal segment of pulmonary surfactant lipopeptide SP-C has intrinsic propensity to interact with and perturb phospholipid bilayers. *Biochem. J.* 377:183–193.

Poulain, F. R., and J. A. Clements. 1995. Pulmonary surfactant therapy. *West. J. Med.* 162:43–50.

Robertson, B., and H. L. Halliday. 1998. Principles of surfactant replacement. *Biochim. Biophys. Acta.* 1408:346–361.

Saulnier, P., F. Foussard, F. Boury, and J. E. Proust. 1999. Structural properties of asymmetric mixed-chain phosphatidylethanolamine films. *J. Colloid Interface Sci.* 218:40–46.

Schief, W. R., M. Antia, B. M. Discher, S. B. Hall, and V. Vogel. 2003. Liquid-crystalline collapse of pulmonary surfactant monolayers. *Biophys. J.* 84:3792–3806.

Schürch, S., R. Qanbar, H. Bachofen, and F. Possmayer. 1995. The surface-associated surfactant reservoir in the alveolar lining. *Biol. Neonate.* 1:61–76.

Smaby, J. M., M. M. Momsen, H. L. Brockman, and R. E. Brown. 1997. Phosphatidylcholine acyl unsaturation modulates the decrease in interfacial elasticity induced by cholesterol. *Biophys. J.* 73:1492–1505.

Somerharju, P. J., J. A. Virtanen, K. K. Eklund, P. Vainio, and P. K. Kinnunen. 1985. 1-Palmitoyl-2-pyrenedecanoyl glycerophospholipids as membrane probes: evidence for regular distribution in liquid-crystalline phosphatidylcholine bilayers. *Biochemistry.* 24:2773–2781.

Sparr, E., K. Ekelund, J. Engblom, S. Engström, and H. Wennerström. 1999. An AFM study of lipid monolayers. Effect of cholesterol on fatty acid. *Langmuir.* 1999:6950–6955.

Tanaka, K., A. P. Manning, V. K. Lau, and H. Yu. 1999. Lipid lateral diffusion in dilauroylphosphatidylcholine/cholesterol mixed monolayers at the air/water interface. *Langmuir.* 15:600–606.

Taneva, S., and K. M. W. Keough. 1997. Cholesterol modifies the properties of surface films of dipalmitoylphosphatidylcholine plus pulmonary surfactant-associated protein B or C spread or adsorbed at the air-water interface. *Biochemistry.* 36:912–922.

Vandenbussche, G., A. Clercx, T. Curstedt, J. Johansson, H. Jornvall, and J. M. Ruysschaert. 1992. Structure and orientation of the surfactant-associated protein C in a lipid bilayer. *Eur. J. Biochem.* 203:201–209.

Veldhuizen, E. J., and H. P. Haagsman. 2000. Role of pulmonary surfactant components in surface film formation and dynamics. *Biochim. Biophys. Acta.* 1467:255–270.

Veldhuizen, R., K. Nag, S. Orgeig, and F. Possmayer. 1998. The role of lipids in pulmonary surfactant. *Biochim. Biophys. Acta.* 1408:90–108.

Virtanen, J. A., M. Ruonala, M. Vauhkonen, and P. Somerharju. 1995. Lateral organization of liquid-crystalline cholesterol-dimyristoylphosphatidylcholine bilayers. Evidence for domains with hexagonal and centered rectangular cholesterol superlattices. *Biochemistry.* 34:11568–11581.

Vist, M. R., and J. H. Davis. 1990. Phase equilibria of cholesterol/dipalmitoylphosphatidylcholine mixtures: 2H nuclear magnetic resonance and differential scanning calorimetry. *Biochemistry.* 29:451–464.

von Nahmen, A., A. Post, H.-J. Galla, and M. Sieber. 1997. The phase behaviour of lipid monolayers containing pulmonary surfactant protein C studied by fluorescence light microscopy. *Eur. Biophys. J.* 26:359–369.

Vorbroker, D. K., S. A. Profitt, L. A. Nogee, and J. A. Whitsett. 1995. Aberrant processing of surfactant protein C in hereditary SP-B deficiency. *Am. J. Physiol.* 268:L647–L656.

Worthman, L. A., K. Nag, P. J. Davis, and K. M. Keough. 1997. Cholesterol in condensed and fluid phosphatidylcholine monolayers studied by epifluorescence microscopy. *Biophys. J.* 72:2569–2580.

Yu, S. H., and F. Possmayer. 1996. Effect of pulmonary surfactant protein A and neutral lipid on accretion and organization of dipalmitoylphosphatidylcholine in surface films. *J. Lipid Res.* 37:1278–1288.

Yu, S. H., and F. Possmayer. 1998. Interaction of pulmonary surfactant protein A with dipalmitoylphosphatidylcholine and cholesterol at the air/water interface. *J. Lipid Res.* 39:555–568.

Yuan, C., and L. J. Johnston. 2000. Distribution of ganglioside GM1 in L-α-dipalmitoylphosphatidylcholine/cholesterol monolayers: a model for lipid rafts. *Biophys. J.* 79:2768–2781.